

## Graphene sponge for efficient and repeatable adsorption and desorption of water contaminations†

Jinping Zhao, Wencai Ren\* and Hui-Ming Cheng

Received 26th June 2012, Accepted 10th August 2012

DOI: 10.1039/c2jm34128j

Seeking highly-efficient, low-cost and robust methods to disinfect and decontaminate water from source to point-of-use is very much in demand. Here, we developed a new material, graphene sponge (GS), for water treatment, which was assembled with graphene oxide sheets by hydrothermal treatment with the assistance of thiourea. These GSs show a tunable pore structure and surface properties, and are mechanically strong. They show high adsorption ability for various water contaminations such as dyes, oils and many other organic solvents. The adsorption capacity of methylene blue and diesel oil in GSs can reach 184 mg g<sup>-1</sup> and 129 g g<sup>-1</sup>, respectively. Moreover, the GSs can be repeatedly used by simple treatment without obvious structure and performance degradation. Additionally, we studied the relationship between the structure and contamination adsorption performance of GSs. It was found that the dye adsorption performance of GSs strongly depends on their surface charge concentration and specific surface area, but the oil adsorption capacity is mainly related to their specific surface area, indicating the different adsorption mechanism. These findings open up many possibilities for the use of graphene in water cleaning, including disinfection, decontamination, re-use, reclamation and desalination.

## Introduction

One of the most pervasive problems throughout the world is inadequate access to clean water and sanitation.<sup>1</sup> Nowadays, in both developing and developed countries, a growing number of contaminants including heavy metals, oils and dyes are entering water supplies from human activities. Therefore, seeking highly-efficient, low-cost and robust methods to disinfect and decontaminate water from source to point-of-use is very much in demand.<sup>1</sup> Dyes are usually used to color products in industries, and are one kind of major contaminations in water. From an environmental point of view, the removal of synthetic dyes is of great concern, since some dyes and their degradation products may be carcinogens and toxic.<sup>2</sup> Oil is another serious contamination, which can cause widespread pollution in sea and coastal waters.<sup>3,4</sup> Among the currently developed treatment methods, such as coagulation, flocculation, biological treatment and adsorption, the latter is extensively growing in use for water treatment due to its ability to remove different types of contaminations and to provide high-quality water, and ease of

operation.<sup>5</sup> The materials for adsorption must have a high specific surface area and chemical stability, so carbon materials are a good candidate for adsorption. Currently, many kinds of carbon materials have been developed to remove water contaminations, such as activated carbon,<sup>2,6–9</sup> activated carbon fibers,<sup>10–12</sup> and carbon nanotubes (CNTs).<sup>13–17</sup>

Graphene is a new carbon material with a two-dimensional structure and many excellent properties.<sup>18–21</sup> The high specific surface area (theoretically ~2600 m<sup>2</sup> g<sup>-1</sup>) and good chemical stability make graphene a good material for adsorption treatment of polluted water. However, graphene is hydrophobic and tends to aggregate due to the van der Waals interactions between neighbouring sheets in water. Aggregation leads to great reduction in the surface area, and is not beneficial for the adsorption of contaminants. Moreover, the affinity of materials to adsorb molecules is mainly determined by H-bonding, van der Waals interactions,  $\pi$ - $\pi$  interactions and electrostatic interaction between them.<sup>22–25</sup> Therefore, proper chemical modification of graphene is required to make it water soluble and have suitable surface properties to improve its adsorption capacity. In addition, high structural stability during the adsorption and desorption processes is also required so that it can be collected easily and used repeatedly, avoiding recontamination of the treated water. Graphene oxide (GO) is an important derivative of graphene and can be produced on a large scale and at low cost by chemical exfoliation of graphite.<sup>26–29</sup> The presence of many oxygen-containing functional groups makes it water soluble and easily chemically modified, which can consequently improve the

Shenyang National Laboratory for Materials Science, Institute of Metal Research, Chinese Academy of Sciences, Shenyang 110016, P. R. China. E-mail: wcren@imr.ac.cn

† Electronic supplementary information (ESI) available: Photographs of rhodamine B solution after GO powders adsorption, SEM images, XPS spectra and BET data of different GSs, molecular formula of different dyes, adsorption performance comparison of GSs with other materials. See DOI: 10.1039/c2jm34128j

accessibility and affinity of GO to adsorbate molecules. For example, pristine GO powders show high dye adsorption performance (Fig. S1†), but unfortunately they cannot be easily collected and separated from treated water, leading to serious recontamination. It is worth noting that most of the developed adsorbents also exist as powders,<sup>30–39</sup> and have the same problems with GO powders.

In this study, we developed a new method to reduce and modify GO sheets and assemble them into graphene sponges (GSs). The GSs obtained have a tunable pore structure and surface properties, and are mechanically robust. They show excellent adsorption and desorption performance for various water contaminations such as dyes, oils and many other organic solvents, and can be repeatedly used many times without obvious structure and performance degradation. We also studied the relationship between the structure and contamination adsorption performance of GSs. It was found that the dye adsorption performance of GSs strongly depends on their surface charge concentrations and specific surface area, but oil adsorption capacity is mainly related to their specific surface area, indicating the different adsorption mechanism.

## Experimental

### Preparation of GSs

Large and small GO sheets were prepared by modified chemical exfoliation,<sup>29</sup> using natural flake graphite with a size of 500–600  $\mu\text{m}$  and natural flake graphite powders with a size of 40–60  $\mu\text{m}$  as raw materials, respectively. The GSs were fabricated by hydrothermal treatment of GO suspensions with the assistance of thiourea. Firstly, a specific amount of thiourea was added into 50 ml homogeneous GO aqueous dispersion, and then the mixture was sealed in a 80 ml Teflon-lined stainless steel autoclave and maintained at 180  $^{\circ}\text{C}$  for 4.5 h. After that, the graphene assembly was dipped into distilled water for 24 h to remove the residual thiourea. Finally, vacuum freeze-drying was used to remove water and obtain GSs. In order to tune the structure and surface properties of GSs, we changed the thiourea quantity, concentration of GO solution and the size of GO sheets during the hydrothermal treatment process. Table S1† shows five different experimental conditions and the corresponding GS products, which are denoted as GS1, GS2, GS3, GS4 and GS5.

### Characterization of GSs

The structure of GSs before and after adsorption as well as after desorption was characterized by SEM (FEI Nova NanoSEM 430, 15 kV), and their composition and surface properties were evaluated by XPS (ESCALAB 250 using focused monochromatized Al K radiation (1486.6 eV)).

### Dye adsorption and desorption

Taking rhodamine B ( $\text{C}_{28}\text{H}_{31}\text{ClN}_2\text{O}_3$ , relative molecular mass: 479) as an example, a GS was first put into a rhodamine B solution (100 ml, concentration:  $2 \times 10^{-4} \text{ mol l}^{-1}$ ), and then the solution was stirred at 25  $^{\circ}\text{C}$  until the color did not change. During the stirring process, the concentration of rhodamine B was measured every half an hour using a UV-vis

spectrophotometer (JASCO V-550). For desorption, the GS adsorbed with rhodamine B was put into ethanol. With shaking, the adsorbed rhodamine B gradually desorbed from the GS and changed the color of ethanol to pink. After the ethanol solution became colorless by repeated washing with ethanol, the GS was dried by vacuum freeze-drying for repeated use.

The dye adsorption amount within time  $t$  (min),  $q_t$  ( $\text{mg g}^{-1}$ ), was calculated by  $q_t = (C_0 - C_t)V/W$ .<sup>2</sup> Here,  $C_0$  and  $C_t$  ( $\text{mg l}^{-1}$ ) are the liquid-phase concentration of dyes at the beginning and after time  $t$  (min), respectively.  $V$  (l) is the volume of the solution, and  $W$  (g) is the mass of the GS used.

### Oil and other organics adsorption

We measured the adsorption capacity ( $Q$ ) of GSs for various organic solvents with different densities, including *n*-heptane (density =  $0.68 \text{ g cm}^{-3}$ ), ethanol ( $0.78 \text{ g cm}^{-3}$ ), diesel oil ( $0.84 \text{ g cm}^{-3}$ ), acetic ester ( $0.90 \text{ g cm}^{-3}$ ), vegetable oil ( $0.89 \text{ g cm}^{-3}$ ), ethylene glycol ( $1.11 \text{ g cm}^{-3}$ ) and chloroform ( $1.48 \text{ g cm}^{-3}$ ). The GS was first put into the organic solvents for 10 min. After picking out, the weights of the sponge before ( $\text{wt GS}_{\text{before}}$ ) and after ( $\text{wt GS}_{\text{after}}$ ) adsorption were measured for  $Q$  calculation with the equation  $Q = (\text{wt GS}_{\text{after}} - \text{wt GS}_{\text{before}})/\text{wt GS}_{\text{before}}$ .

### Zeta potential measurement

The GS was first crushed into powders. Then, 0.01 g GS powder, 1 ml Triton X-100 and 40 ml distilled water were mixed in a beaker, and the mixture was dispersed by a tip sonicator (SCI-ENTZ-IID) for 1 h. The obtained uniform graphene dispersion was used to measure the Zeta potential by ZETASIZER Nano series, Nano-ZS90.

## Results and discussion

### Preparation and characterization of GSs

The GO sheets were prepared by modified chemical exfoliation, as we reported previously.<sup>29</sup> They are predominantly monolayers (more than 95%), and have a size ranging from hundreds of nanometers to 100  $\mu\text{m}$ , depending on the experimental conditions

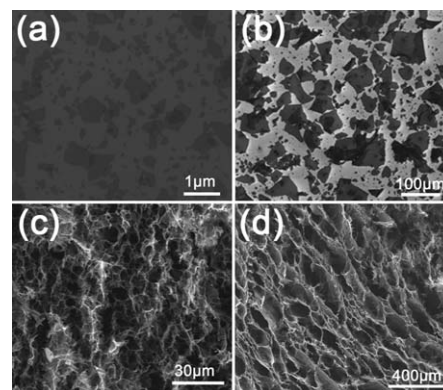


**Fig. 1** Structure of GSs. (a) and (b) SEM images of (a) small GO sheets (about several hundred nanometers) and (b) large GO sheets (up to 100  $\mu\text{m}$ ). (c) and (d) SEM images of GSs prepared by (c) small GO sheets in (a) and (d) large GO sheets in (b), showing their porous structure.

(Fig. 1a and b). The GSs were prepared by a hydrothermal process. Briefly, thiourea was first added into a homogeneous GO aqueous dispersion, and then the mixture was sealed in a container and maintained at 180 °C for 4.5 h, followed by vacuum freeze-drying. The materials obtained show a porous structure (Fig. 1c and d), which allows for a high specific surface area for contamination adsorption, and behaves like a sponge, so they are called GSs. The pore size and specific surface area of GSs can be tuned by changing the size of GO sheets and the concentration of GO solution. For example, under a high GO solution concentration of 2 mg ml<sup>-1</sup>, the GSs (GS3) made by small GO sheets with a size of hundreds of nanometers show a pore size of about several microns and a specific surface area of 150 m<sup>2</sup> g<sup>-1</sup> (Fig. 1c and Table S1†), and the GSs (GS5) made by large GO sheets with a size up to 100 μm show a pore size of hundreds of microns and a specific surface area of 79 m<sup>2</sup> g<sup>-1</sup> (Fig. 1d and Table S1†). By using a low concentration of GO solution (1 mg ml<sup>-1</sup>, GO size: hundreds of nanometers), we can get GSs (GS4) with a surface area of 399 m<sup>2</sup> g<sup>-1</sup> (Table S1 and Fig. S2†).

Interestingly, the GSs show excellent mechanical properties, very good processability and structural stability. It can be seen that the sponges can be cut into different shapes without any breaking and a pore structure change (Fig. 2a). A small GS (GS3, see Table S1†) with a diameter of 22.9 mm and thickness of 11.9 mm can support a counterweight of 500 g without any deformation (Fig. 2b). The maximum compression stress that a sponge (GS4, see Table S1†) is able to sustain before structure degradation can reach 140 kPa with a strain of ~82% (Fig. 2c).

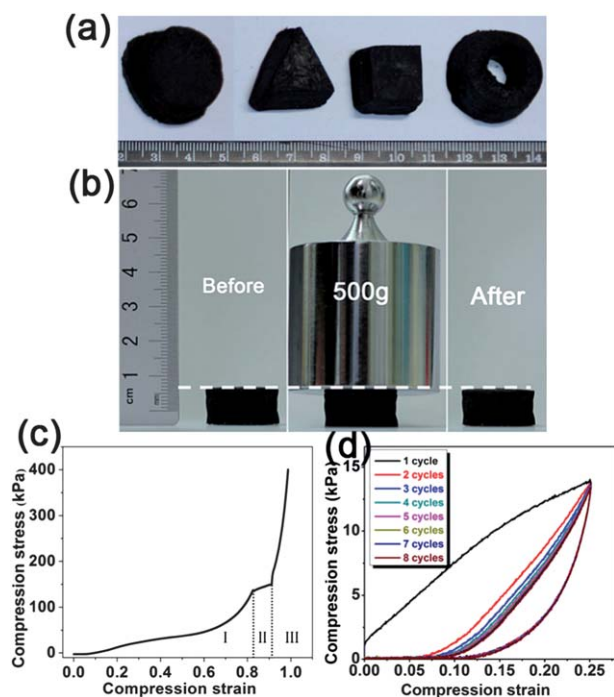


**Fig. 2** (a) Optical images of GSs cut with different shapes, showing their high structural stability and good processability. (b) Optical images of a GS before loading, loaded and after unloading a counterweight, showing its good mechanical property. (c) Stress–strain curve for a GS with a diameter of 23.6 mm and a thickness of 12.7 mm. (d) Cyclic stress–strain curves for the same GS at a maximum compression strain of 25% in air.

Moreover, the sponge shows good cyclic performance under loading and unloading compression. It maintains similar compression stress (14 kPa) at the maximum strain (~25%) in each cycle, and can almost recover to its original structure after releasing the compression (Fig. 2d). The good mechanical property indicates strong interactions between the neighboring sheets in sponges. Such good processability, elasticity and structural stability allow repeated use of GSs for contamination adsorption and desorption without the risk of recontamination to the treated water.

The use of thiourea plays important roles in the formation of porous and strong GSs. During the hydrothermal process, thiourea was decomposed to ammonia, hydrogen sulfide and other compounds. On the one hand, these gases can make the GO sheets separated. On the other hand, the reaction between GO sheets and thiourea can not only reduce the GO sheets but can also form many new functional groups such as amino (–NH<sub>2</sub>) and sulfonic acid (–SO<sub>3</sub>H) (Fig. S3, S4 and Table S2†). Similar to oxygen functional groups,<sup>40</sup> these newly formed functional groups binding on the graphene surface act as roughness at the atomic scale to enable a strong crosslink between the neighboring sheets, and consequently, the GO sheets were assembled into compact porous sponges with good structural stability. Moreover, according to Raman measurements, the graphene sheets in sponges changed from amorphous states to more graphitic structures after thiourea treatment (Fig. S5†). In contrast, without the use of thiourea, only small GSs with a smaller specific surface area were formed for the same quantity of GO solution, in which GO sheets are strongly aggregated (Fig. S6†). Moreover, such sponges show a loose structure with many large pores that can be seen by the eye.

### Dyes adsorption and desorption in GSs

We studied the adsorption of GSs to three typical dyes, methylene blue, rhodamine B and methyl orange (Fig. S7†). Here, the GS3 (Table S1†) with a specific surface area of 150 m<sup>2</sup> g<sup>-1</sup> was used. It is worth noting that the GSs show good adsorption ability to these three dyes (concentration: 2 × 10<sup>-4</sup> mol l<sup>-1</sup>), although the adsorption amounts and rates are different (Fig. S8†). Methylene blue and rhodamine B can be mostly removed from water typically within 4 h, which is much faster than the adsorption of methyl orange (24 h). Methylene blue shows the highest adsorption amount (about 184 mg g<sup>-1</sup>) among the three dyes, but cannot be desorbed easily. Methyl orange shows the lowest adsorption amount of 11.5 mg g<sup>-1</sup>. Rhodamine B also shows a high adsorption amount (72.5 mg g<sup>-1</sup>), and can be easily desorbed from the GSs in methanol or ethanol, which suggests repeatable use of GSs for removing rhodamine B from water. Therefore, we chose rhodamine B as a representative adsorbate to study the adsorption and desorption processes in GSs as well as the effect of the sponge structure on adsorption capacity.

Fig. 3 shows the adsorption and desorption of rhodamine B in GSs. It can be found that, after putting a GS into rhodamine B water solution (concentration: 2 × 10<sup>-4</sup> mol l<sup>-1</sup>) for 180 min, the pink solution turned colorless and the characteristic absorption peak of rhodamine B disappeared (Fig. 3b and S9†), indicating the removal of rhodamine B. When we put the GS adsorbed with rhodamine B into ethanol, the colorless ethanol solution became

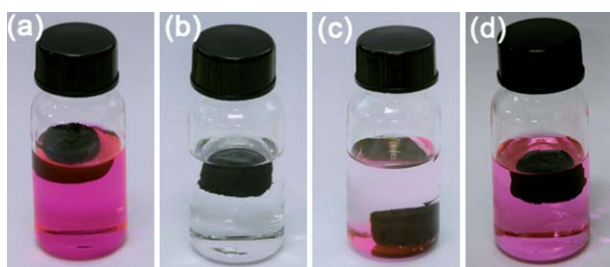


**Fig. 3** The adsorption and desorption of rhodamine B in GS. (a) and (b) A GS in rhodamine B solution (a) at the beginning and (b) for 180 min. (c) and (d) The same GS adsorbed with rhodamine B in ethanol for (c) 2 min and (d) 10 min.

light pink (Fig. 3c) after about 2 min and finally turned to dark pink (Fig. 3d) after about 10 min, indicating that rhodamine B was gradually released from the GS. Rhodamine B can be removed completely after repeated washing with ethanol several times. Moreover, we found that other solvents like methanol and carboxylic acids can also be used to desorb rhodamine B from GSs.

Fig. 4a shows that the GSs have a very good adsorption performance towards rhodamine B with an adsorption amount of  $72.5 \text{ mg g}^{-1}$  and equilibrium time of 180 min for GS3. As shown in Table S3†, this performance is much better than that of reduced GO,<sup>24</sup> magnetite/reduced GO composites<sup>30</sup> and many other materials such as multi-walled CNTs,<sup>31</sup> CNTs/activated carbon fiber composites,<sup>32</sup> materials derived from agriculture and industry waste<sup>33–35</sup> and hypercrosslinked polymeric adsorbents,<sup>36</sup> and is comparable to those of activated carbon (20 to  $400 \text{ mg g}^{-1}$  depending on its structure).<sup>37–39</sup> Another very important feature for the use of GSs for dye adsorption is that the GSs can be repeatedly used without obvious performance degradation.

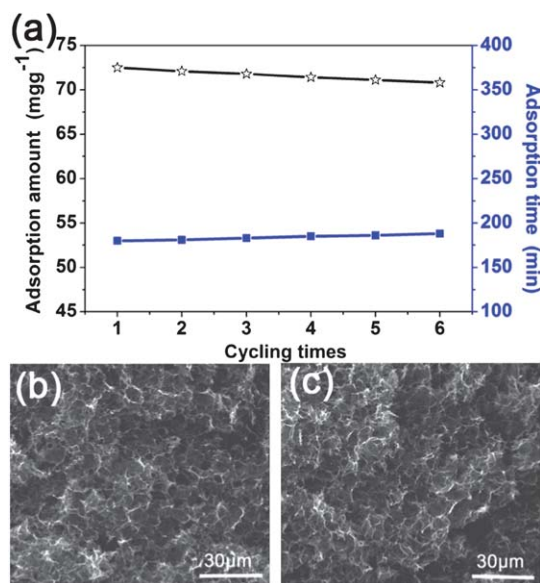


**Fig. 4** Cyclic performance of GSs for dye adsorption. (a) Adsorption amount and the corresponding adsorption time of rhodamine B for different cycles. (b) and (c) SEM image of a GS after (b) adsorption and (c) desorption of rhodamine B.

From Fig. 4a, it can be found that the decrease in the adsorption amount of rhodamine B is less than 2.3% and the corresponding adsorption time is increased less than 4% after 6 adsorption and desorption cycles. Moreover, it is worth noting that the GS completely keeps its original structure after adsorption (Fig. 4b) and desorption (Fig. 4c), which is believed to be responsible for its high cycling stability shown above. Even after adsorption/desorption operation many times, no visible graphene sheets were observed in the treated water and no detectable weight loss was observed in the GS as well, avoiding the recontamination problem faced by powder-like adsorbents.

In order to tune the surface properties and elucidate the adsorption mechanism of GSs, we changed the thiourea quantity (0.1, 0.3, 0.5 g) used during the GS preparation process to obtain different samples, which are denoted as GS1, GS2, and GS3, respectively (Table S1†). Here, 50 ml GO solution (GO size: hundreds of nanometers) with a concentration of  $2 \text{ mg ml}^{-1}$  was used. We also tried to use higher thiourea quantity, but unfortunately the sponges became loose with decreased processability and structure stability. For example, only deformed GSs were obtained when 0.7 g thiourea was used (Fig. S10†). Fig. 5a shows that the rhodamine B adsorption performance of GSs increases with increasing the thiourea quantity. The highest adsorption amount is 54.6, 63.3 and  $72.5 \text{ mg g}^{-1}$  for GS1, GS2 and GS3, respectively, with the corresponding equilibrium time of 360, 300 and 180 min. Fig. 5b shows the rhodamine B adsorption kinetics of different kinds of GSs. The good linear relationship of  $t/q_t$  ( $t$  is the adsorption time,  $q_t$  is the adsorption amount within  $t$ ) versus  $t$  suggests that the adsorption of rhodamine B on GSs predominantly follows the pseudo-second-order kinetic model.<sup>9</sup> The higher adsorption rate constant ( $k$ ) of GS3 (0.19) than that of GS1 (0.06) and GS2 (0.08) further confirms the higher adsorption performance of GS3.

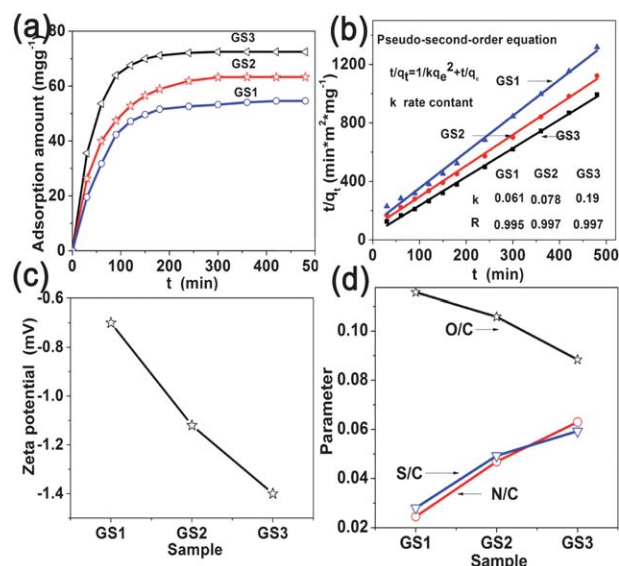


**Fig. 5** Adsorption performance and surface properties of different GSs. (a) Adsorption amount of rhodamine B as a function of adsorption time. (b) Adsorption kinetics of rhodamine B, (c) Zeta potential, and (d) O/C, N/C and S/C atomic ratio of three different GSs prepared with different thiourea amounts.

The adsorption capacity of a material is usually influenced by the pore size, specific surface area, surface charges, and particle size of the adsorbents and the dimension of adsorbate molecules.<sup>9,41</sup> In order to understand the adsorption mechanism of GS for dyes, we measured the pore structure and specific surface area of GS1, GS2 and GS3, and the results are shown in the ESI (Fig. S11 and Table S1†). It can be found that there is only a little difference in the pore size and specific surface area. Therefore, we suggest that the big difference in adsorption capacity of GS1, GS2 and GS3 is mainly attributed to the difference in their surface properties.

Zeta potential is an important parameter to evaluate the charge amount on the surface of a material.<sup>42</sup> We measured the Zeta potential of GS1, GS2 and GS3 in distilled water. Triton X-100 is a non-ionic surfactant, and does not produce charges in water. Therefore, Triton X-100 was used to disperse GSs for Zeta potential measurements. Fig. 5c shows the Zeta potential of GS1, GS2 and GS3. It is worth noting that all the GSs are negatively charged, and the absolute value of Zeta potential is 0.7, 1.1 and 1.4 mV for GS1, GS2 and GS3, respectively. Therefore, we suggest that the electrostatic interaction plays an important role in the dye adsorption in GSs. The more negative the charges GSs, the higher the adsorption capacity and the faster the desorption rate of rhodamine B, since rhodamine B is positively charged (Fig. S7†).

To reveal the reason behind the Zeta potential difference of different GSs, we analyzed their surface properties based on XPS measurements. Note that thiourea not only reduced the GO sheets, but also created some N- and S-containing functional groups such as amino and sulfonic acid (Fig. S3, S4 and Table S2†). Fig. 5d shows the O/C, N/C and S/C atomic ratio of different GS samples. It can be found that the O/C ratio decreases and the N/C and S/C ratio increases at the same time, when more thiourea is used (Fig. 5d and Table S2†). This means that more C–O bonds were broken with oxygen removed, and more N- and S-containing functional groups were formed. These newly formed functional groups also make the graphene sheets negatively charged because of the charge transfer, so the GS3 sample is more negatively charged than GS1 and GS2. These results indicate that the charge condition on the surface of GSs can be tuned by chemical modification.

Another thing we need to point out is that methyl orange in water can also be absorbed by negatively charged GSs (Fig. S8†) even though it is negatively charged (Fig. S7†). This result indicates that the van der Waals interaction is another cause for the dye adsorption. For both the electrostatic interaction adsorption and the van der Waals interaction adsorption, the specific surface area of the sponge plays an important role in its adsorption capacity since the sponge with a higher surface area has more charges and surface for dye adsorption. We compared the rhodamine B adsorption performance of GSs with similar Zeta potential but a different specific surface area. As expected, the larger the specific surface area, the larger the adsorption capacity (Table S4†). Different from the commonly used carbon materials for dye adsorption, our GSs not only have a rich pore structure and a high specific surface area but also have many charges on their surface. Therefore, they show superior adsorption performance to many other materials, as shown in Table S3†. We believe that the adsorption performance of GSs can be further tuned and improved by structure design and suitable surface modification.

## Various oils and organics absorption and desorption in GSs

Besides dyes, we also demonstrated the use of GSs for adsorption of various oils and many other organics. The GSs used were prepared by using a low concentration of GO solution (GS4, see Table S1†). Here, adsorption capacity ( $Q$ ) was used to evaluate the adsorption performance of GSs, which is defined by the weight ratio of the adsorbed organics to the pristine GSs. It can be found from Fig. 6a that organics with higher density have larger  $Q$ . Among all the investigated organics, chloroform shows the largest  $Q$  of  $154 \text{ g g}^{-1}$ . We also compared the oil adsorption capacity of GSs with many other materials,<sup>17,43</sup> including CNT sponge, polyurethane sponge, loofah skeleton, degreasing cotton, activated carbon, polyester sponge and nanowires (Fig. 6b). The data show that the adsorption capacity of GSs for diesel oil is comparable to that of CNT sponge and much higher than those of other materials. Compared to the CNT sponges prepared by high-temperature chemical vapor deposition, our GSs prepared by hydrothermal treatment have the advantages of a low cost and easily tuned structure and surface properties. The GSs can also be used to absorb the diesel oil floating on the water. Note that 2 g of diesel oil on water can be absorbed by GSs in 10 s (Fig. 6c–e). Moreover, it is worth noting that the adsorbed oil and other organic solvents can be easily removed by burning in air without destroying the sponge structure (Fig. 7). The repeatedly used GSs also show very good cycling performance for the adsorption of diesel oil and ethanol (Fig. S12†).

We also found that GS1, GS2 and GS3 show almost no difference in the adsorption capacity for diesel oil (GS1:  $81 \text{ g g}^{-1}$ , GS2:  $84 \text{ g g}^{-1}$ , and GS3:  $84 \text{ g g}^{-1}$ ). This means that the adsorption capacity of GSs for diesel oil does not depend on the quantity of the charges on the GSs surface, which is different from the adsorption of dyes. Note that the GSs with a specific surface area of  $399 \text{ m}^2 \text{ g}^{-1}$  shows a diesel oil adsorption capacity

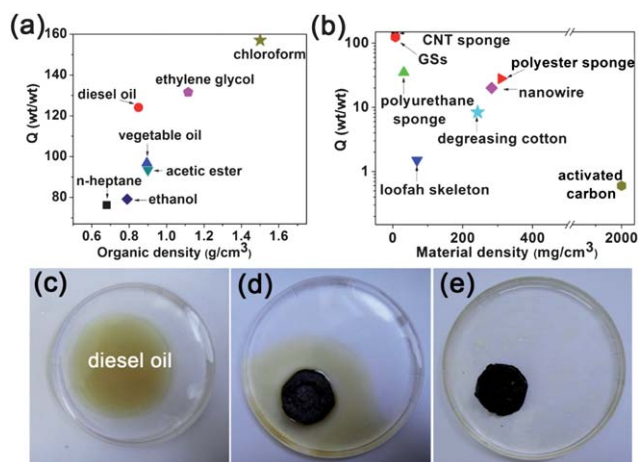


**Fig. 6** Adsorption of GSs for various organics. (a) Adsorption capacity ( $Q$ ) of GSs for oils and many other organics. (b) Diesel oil adsorption capacity of GSs and many other materials,<sup>17,43</sup> including CNT sponge, polyurethane sponge, loofah skeleton, degreasing cotton, activated carbon, polyester sponge and nanowires. (c)–(e) Illustration of the adsorption of GSs for diesel oil. (c) A drop of diesel oil on water. (d) and (e) A GSs in the diesel oil solution (d) at the beginning and (e) for 10 s. Note that the diesel oil was absorbed by the GSs after 10 s.

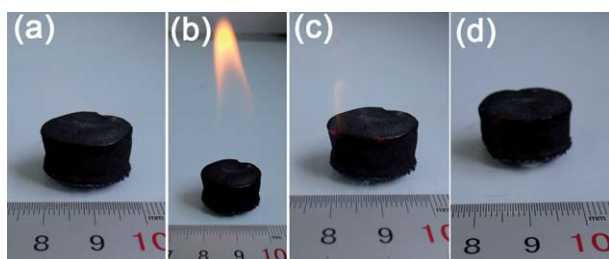


**Fig. 7** Removal of ethanol in GSs by burning for repeated use. (a) A GS after full adsorption of ethanol. (b)–(d) Burning of the ethanol in GS (b) at the beginning, (c) for 30 s, and (d) for 60 s. Note that the ethanol was burnt completely after 60 s, and the structure of the GS was not destroyed.

of about  $129 \text{ g g}^{-1}$ , which is much larger than that ( $84 \text{ g g}^{-1}$ ) of a sponge with a specific surface area of  $150 \text{ m}^2 \text{ g}^{-1}$ . Therefore, we consider that the adsorption of GSs for oils is mainly based on van der Waals interactions, and is strongly related to the specific surface area of the GSs.

## Conclusions

We have modified GO sheets and assembled them into GSs by the hydrothermal treatment with the assistance of thiourea. These GSs show a tunable pore structure and surface properties, and are mechanically strong. They show high adsorption ability for various water contaminations such as dyes, oils and many other organic solvents. The GSs can also be repeatedly used without obvious structure and performance degradation. Additionally, we studied the relationship between the structure and contamination adsorption performance of GSs. It was found that the dye adsorption performance of GSs strongly depends on their surface charge concentrations and specific surface area, but the oil adsorption capacity is mainly related to their specific surface area, indicating the different adsorption mechanism. These findings open up many possibilities for the use of graphene in water cleaning, including disinfection, decontamination, reuse, reclamation and desalination.

## Acknowledgements

This work was supported by the National Science Foundation of China (nos. 51172240, 50921004 and 50972147) and the Ministry of Science and Technology of China (no. 2012AA030303). The authors thank Dr F. Li, Dr L.B. Gao, Mr Z. Weng and Mr Z.P. Chen for their kind help.

## Notes and references

- M. A. Shannon, P. W. Bohn, M. Elimelech, J. G. Georgiadis, B. J. Marinas and A. M. Mayes, *Nature*, 2008, **452**, 301.
- B. H. Hameed, A. L. Ahmad and K. N. A. Latiff, *Dyes Pigm.*, 2007, **75**, 143.
- M. O. Adebajo, R. L. Frost, J. T. Klopogge, O. Carmody and S. Kokot, *J. Porous Mater.*, 2003, **10**, 159.
- X. C. Gui, H. B. Li, K. L. Wang, J. Q. Wei, Y. Jia, Z. Li, L. L. Fan, A. Y. Cao, H. W. Zhu and D. H. Wu, *Acta Mater.*, 2011, **59**, 4798.

- A. W. M. Ip, J. P. Barford and G. McKay, *J. Colloid Interface Sci.*, 2009, **337**, 32.
- I. A. W. Tan, A. L. Ahmad and B. H. Hameed, *J. Hazard. Mater.*, 2008, **154**, 337.
- I. A. W. Tan, A. L. Ahmad and B. H. Hameed, *Desalination*, 2008, **225**, 13.
- S. Karaca, A. Gurses, M. Acikyildiz and M. Ejder, *Microporous Mesoporous Mater.*, 2008, **115**, 376.
- D. W. Wang, F. Li, G. Q. Lu and H. M. Cheng, *Carbon*, 2008, **46**, 1593.
- S. J. Zhang, T. Shao, H. S. Kose and T. Karanfil, *Environ. Sci. Technol.*, 2010, **44**, 6377.
- S. Kumagai, H. Ishizawa and Y. Toida, *Fuel*, 2010, **89**, 365.
- F. Y. Yi, X. D. Lin, S. X. Chen and X. Q. Wei, *J. Porous Mater.*, 2008, **16**, 521.
- Q. F. Liu, W. C. Ren, D. W. Wang, Z. G. Chen, S. F. Pei, B. L. Liu, F. Li, H. T. Cong, C. Liu and H. M. Cheng, *ACS Nano*, 2009, **3**, 707.
- Y. M. Yan, M. N. Zhang, K. P. Gong, L. Su, Z. X. Guo and L. Q. Mao, *Chem. Mater.*, 2005, **17**, 3457.
- K. S. Lin, H. W. Cheng, W. R. Chen and C. F. Wu, *Adsorption*, 2010, **16**, 47.
- M. M. Ayad and A. Abu El-Nasr, *J. Phys. Chem. C*, 2010, **114**, 14377.
- X. C. Gui, J. Q. Wei, K. L. Wang, A. Y. Cao, H. W. Zhu, Y. Jia, Q. K. Shu and D. H. Wu, *Adv. Mater.*, 2010, **22**, 617.
- K. S. Novoselov, A. K. Geim, S. V. Morozov, D. Jiang, Y. Zhang, S. V. Dubonos, I. V. Grigorieva and A. A. Firsov, *Science*, 2004, **306**, 666.
- A. K. Geim and K. S. Novoselov, *Nat. Mater.*, 2007, **6**, 183.
- A. K. Geim, *Science*, 2009, **324**, 1530.
- Y. W. Zhu, S. Murali, W. W. Cai, X. S. Li, J. W. Suk, J. R. Potts and R. S. Ruoff, *Adv. Mater.*, 2010, **22**, 3906.
- S. J. Zhang, T. Shao, S. S. K. Bekaroglu and T. Karanfil, *Environ. Sci. Technol.*, 2009, **43**, 5719.
- B. Pan and B. S. Xing, *Environ. Sci. Technol.*, 2008, **42**, 9005.
- G. K. Ramesha, A. V. Kumara, H. B. Muralidhara and S. Sampath, *J. Colloid Interface Sci.*, 2011, **361**, 270.
- M. G. Dai, *J. Colloid Interface Sci.*, 1998, **198**, 6.
- D. R. Dreyer, S. Park, C. W. Bielawski and R. S. Ruoff, *Chem. Soc. Rev.*, 2010, **39**, 228.
- S. Stankovich, D. A. Dikin, G. H. B. Dommett, K. M. Kohlhaas, E. J. Zimney, E. A. Stach, R. D. Piner, S. T. Nguyen and R. S. Ruoff, *Nature*, 2006, **442**, 282.
- T. Ramanathan, A. A. Abdala, S. Stankovich, D. A. Dikin, M. Herrera-Alonso, R. D. Piner, D. H. Adamson, H. C. Schniepp, X. Chen and R. S. Ruoff, *et al.*, *Nat. Nanotechnol.*, 2008, **3**, 327.
- J. P. Zhao, S. F. Pei, W. C. Ren, L. B. Gao and H. M. Cheng, *ACS Nano*, 2010, **4**, 5245.
- H. M. Sun, L. Y. Cao and L. H. Lu, *Nano Res.*, 2011, **4**, 550.
- Y. Yan, H. P. Sun, P. P. Yao, S. Z. Kang and J. Mu, *Appl. Surf. Sci.*, 2011, **257**, 3620.
- L. P. Wang, Z. C. Huang and M. Y. Zhang, *Adv. Mater. Res.*, 2010, **156–157**, 477.
- O. Hamdaoui, *Desalination*, 2011, **271**, 279.
- K. Kadirvelu, C. Karthika, N. Vennilamani and S. Pattabhi, *Chemosphere*, 2005, **60**, 1009.
- M. V. Sureshkumar and C. Namasivayam, *Colloids Surf., A*, 2008, **317**, 277.
- J. H. Huang, K. L. Huang, S. Q. Liu, A. T. Wang and C. Yan, *Colloids Surf., A*, 2008, **330**, 55.
- L. Li, S. X. Liu and T. Zhu, *J. Environ. Sci.*, 2010, **22**, 1273.
- J. Anandkumar and B. Mandal, *J. Hazard. Mater.*, 2011, **186**, 1088.
- Y. P. Qiu, Z. Z. Zheng, Z. L. Zhou and G. D. Sheng, *Bioresour. Technol.*, 2009, **100**, 5348.
- D. A. Dikin, S. Stankovich, E. J. Zimney, R. D. Piner, G. H. B. Dommett, G. Evmenenko, S. T. Nguyen and R. S. Ruoff, *Nature*, 2007, **448**, 457.
- R. Jain, M. Mathur, S. Sikarwar and A. Mittal, *J. Environ. Manage.*, 2007, **85**, 956.
- D. Zadaka, A. Radian and Y. G. Mishael, *J. Colloid Interface Sci.*, 2010, **352**, 171.
- J. K. Yuan, X. G. Liu, O. Akbulut, J. Q. Hu, S. L. Suib, J. Kong and F. Stellacci, *Nat. Nanotechnol.*, 2008, **3**, 332.